Phase Behavior and Mechanism of Formation of Protofiber Morphology of Solution Spun Poly(acrylonitrile) Copolymers in DMF-Water System

Ashwini K. Agrawal, Manjeet Jassal, Anasuya Sahoo, Santhosh K. Garapati

SMITA Labs, Department of Textile Technology, Indian Institute of Technology, Hauz Khas, New Delhi 110016, India

Received 11 August 2007; accepted 31 August 2008
DOI 10.1002/app.32776
Published online 29 July 2010 in Wiley Online Library (wileyonlinelibrary.com).

ABSTRACT: Phase diagrams of a series of copolymers of acrylonitrile (AN) and acrylic acid (AAc) were constructed using linearized cloud point correlation. The miscibility region in the phase diagram was found to increase with the increase in AAc content of the copolymers. For various compositions, χ_{13} (polymer–water interaction parameter) values were estimated by sorption experiment. As the hydrophilic nature of the polymer increased with the increase in the content of acrylic acid, the χ_{13} interaction parameter was found to decrease from poly(acrylonitrile) homopolymer to its copolymer with 50 mol % acrylic acid (AA50B). The polymer–solvent interaction parameters (χ_{23}) and composition at the critical points for all the polymers were determined by fitting the theoretical bimodal curves to the experimental cloud point curves using Kenji Kamide equations. The polymer composition at the critical point was found to increase by 400% with increasing AAc content. The polymers were solution spun in DMF-water coagulation bath at 30°C and their protofiber structures were investigated under scanning electron microscopy. The observed morphological differences in protofibers were explained on the changes brought about in the phase separation behavior of the polymer–solvent–nonsolvent systems. The copolymers with higher acrylic acid content could be solution spun into void free homogeneous fibers even at conditions that produced void-filled inhomogeneous fibers in poly(acrylonitrile) and its copolymers with lower AAc content. The experiments demonstrate the important role of thermodynamics in deciding the protofiber morphology during coagulation process.
 J Appl Polym Sci 119: 837–854, 2011

Key words: phase diagram; protofiber morphology; coagulation; thermodynamics; poly(acrylonitrile); voids; wet spinning

INTRODUCTION

Industrially, wet spinning is a popular process to produce synthetic and regenerated fibers such as acrylic, viscose, acetates, and lyocell, etc. In wet spinning, the homogeneous polymer solution (dope) is extruded through a spinneret into a coagulation bath, where it comes in contact with a coagulant (nonsolvent), which is compatible with solvent but not with the polymer. Because of the existing differences in concentration between the extrudate and the bath (i.e., concentration gradients), the transfer of nonsolvent from coagulation bath to fiber and of solvent from fiber to coagulation bath takes place. The composition of single-phase solution changes gradually until the polymer can not stay in homogeneous solution any longer and starts to phase separate.

The morphology of the protofiber in poly(acrylonitrile) wet spinning system has been studied since early days by several authors to explain the coagulation phenomenon.[1–3] Most of these studies relate morphology to kinetics of coagulation. It has been reported that protofiber assumes a void filled morphology when the rate of coagulation is high. In other words, when rate of diffusion of solvent and nonsolvent is high. This occurs when either the concentration of coagulation bath (i.e., concentration of solvent in solvent–nonsolvent mixture) is low or the temperature of coagulation bath is high, say 30–40°C in PAN–DMF-water system. Therefore, commercially, poly(acrylonitrile) is often wet spun in solvent rich coagulation bath (i.e., high coagulation bath concentration) and at low temperatures in the range of 10–15°C to reduce the number of large voids in the protofiber structure. However, the final state of any system depends on thermodynamics of the process and not the kinetics. Kinetics merely decides the rate at which the equilibrium or the final morphology is obtained. To date, understanding of the effect of various process parameters on the coagulation phenomenon in wet spinning and its relationship to subsequent morphology of the protofibers has not been achieved systematically.

Understanding and control of coagulation phenomenon and the morphology of the protofibers

Correspondence to: A. K. Agrawal (ashwini_agrawal@yahoo.com).

formed is technologically extremely important. The properties of final fiber formed are mainly dependent on the initial protofiber structure formed in the coagulation bath.[4] It has been shown that by generating void free morphology using modified processes such as dry-jet wet spinning, the fibers with significantly better properties can be achieved.[5,6]

Research studies on membrane technology[7–11] have revealed that type of void formation in polymer membranes is normally dictated by the thermodynamics of the phase separation process. During coagulation of microporous films, the thermodynamic factors decide the compositional path the coagulating matrix takes while traversing the binodal curve in the phase diagram, and hence, the mechanism by which phase separation takes place. Therefore, the equilibrium phase diagram is a good tool for controlling the pore morphology and interpreting the membrane structure. Knowledge of phase equilibrium enables one to change the condition for the preparation of membranes such as the temperature and the composition of the polymer solution and of the coagulation bath to obtain desired structure. However, such effects of thermodynamic factors have been generally ignored while studying the coagulation behavior of the wet spun fibers.

It is hoped that the study of the phase diagram of the spinning polymer and the effect of different process parameters on the compositional path that a coagulating fiber may take while crossing the binodal curve, would help in understanding the origin of various types of morphologies that are obtained during wet spinning.

Only a few studies in the literature have attempted to understand the phase behavior of a coagulating fiber.[12–14] In this study, the role of thermodynamic parameters on the structure of wet-spun fibers has been investigated in detail. For this, a series of PAN copolymers with acrylic acid as comonomer were synthesized with changing molecular composition from 0% to 50 mol % of AAc. The effect acrylic acid content on the phase diagram of copolymer–DMF-water system were determined. The copolymers were then wet spun into fibers and the development of morphology at their protofiber stage was related to the process parameters and their effect on coagulation thermodynamics.

EXPERIMENTAL

Materials

Acrylic acid (AAc) and toluene were obtained from Merck India (Mumbai). Acrylonitrile (AN) was purchased from Central Drug House (P) (New Delhi) and initiator α,α'- azobisisobutyronitrile (AIBN) from G. S. Chemical Testing Lab & Allied Industries (New Delhi). Solvents diethyl ether and dimethylformamide (DMF) were obtained from Qualigens Fine Chemicals (Mumbai). All chemicals were of minimum assay of 99% and were used without further purification.

Copolymer synthesis

Homopolymer (PAN)

Free radical copolymerization was carried out in a four-neck reactor in toluene at 65 ± 1°C under nitrogen atmosphere to produce homopolymer of PAN. Two hundred grams of toluene was taken in the reaction flask and degassed for 30 min. The initiator AIBN (0.057 mol %) was dissolved in 40 g of acrylonitrile and degassed for 30 min. It was then added to the reaction flask and the reaction was carried out 4 h. The reaction mixture was cooled and then precipitated in excess diethyl ether to get white polymer. The polymer was washed three times with excess diethyl ether to remove traces of unreacted monomers and toluene. The purified polymer was dried in a vacuum oven at 60°C for 1 h. Gravimetric yield of the polymer was about 35%.

Copolymers (AA10B-AA50B)

Free radical copolymerization was carried out in a four-neck reactor in toluene at 65 ± 1°C under nitrogen atmosphere to produce a series of copolymers with varying acrylic acid (AAc) content in the feed from 10 to 42.7 mol %.[15,16] The total monomer concentration was fixed at 20 wt %. The final AAc content in the feed was varied from 10 to 42.7 mol %. Two hundred grams of toluene was taken in the reaction flask and degassed for 30 min. The initiator AIBN (0.057 mol %) was dissolved in acrylonitrile and degassed for 30 min. It was then added to the reaction flask and the reaction was carried out for 30 min, before starting the addition of acrylic acid (AAc). The more reactive comonomer (AAc) was degassed, and added intermittently in small doses (each dose of 0.9 g added in every 10 min) to the reaction mixture with constant stirring. The reaction was allowed to continue for an additional 30 min. The reaction mixture was cooled and then precipitated in excess diethyl ether to get white copolymer. The copolymers were washed three times with excess diethyl ether to remove traces of unreacted monomers and toluene, followed by repeated washing with excess acetone to remove any homopolymer of acrylic acid. The purified copolymers were dried in a vacuum oven at 60°C for 1 h. Gravimetric yield of the copolymers were about 35%. The various compositions along with copolymer codes are given in Table I.

TABLE I
Viscosity Average Molecular Weight and Composition of PAN and its Copolymers

Copolymer	Acrylic acid feed (mol %)	Intrinsic viscosity (dL/g)	Molecular weight (M_v)	Composition (AAc mol %)	
				By acidimetry	by ^{13}C NMR
Pure PAN	0	3.08	3.61×10^5	0	0
AA50B	42.7	3.07	3.6×10^5	46.05	48.86
AA40B	40	2.94	3.4×10^5	42.14	43.35
AA30B	30	2.81	3.2×10^5	33.00	34.56
AA20B	20	2.94	3.4×10^5	24.64	–
AA10B	10	2.75	3.1×10^5	12.35	–

Copolymer characterization

Intrinsic viscosity

The intrinsic viscosity of the copolymers was determined in DMF using Ubbelohde viscometer in a constant temperature bath at 30 ± 0.1°C. Molecular weight was estimated using Mark-Houwink relation $[\eta] = KM_v^{\alpha}$, where $\alpha = 0.75$ and $K = 20.9 \times 10^{-5}$ dL/g were taken from the literature.[17] The values of intrinsic viscosity for all polymers are given in Table I.

Determination of copolymer composition by ^{13}C NMR spectra

The quantitative ^{13}C NMR spectra of the copolymers were recorded under the standard conditions at 80°C in DMSO-d_6 on a Bruker DPX- 300-MHz Spectrophotometer. The composition of the copolymers was determined by using the peak areas corresponding to carbon atoms in the —COOH of acrylic acid and —CN groups of acrylonitrile. The composition of the copolymer was calculated by the formula.

$$\text{Mole percent of acrylonitrile} = \frac{I_{CN}}{I_{CN} + I_{CO}}$$

where I_{CN} is the intensity of CN and I_{CO} is the intensity of CO as noted from the ^{13}C quantitative NMR.[18]

Acidimetric titration

The 0.5 wt % solutions of copolymers in DMF were titrated against 0.05*N* aqueous NaOH (standardized) using a phenolphthalein as an indicator as per the reported method for copolymers of acrylonitrile and acrylic acid.[19]

Fiber spinning

The dope solutions containing 10 and 20 wt % polymer were prepared by stirring the purified and dried polymer powder in DMF. The solutions were kept in vacuum at the room temperature to allow deaeration before spinning. Fibers were extruded using a syringe type monofilament extruder into a coagulation bath containing 10 and 30% (by volume) of DMF in water maintained at 30°C. The extruded protofibers were drawn to a draw ratio of 2.0 during the coagulation process.

Fiber morphology using scanning electron microscopy

Morphology of the protofibers, obtained just after coagulation bath was observed under scanning electron microscope (Zeiss EVO 50) at magnifications of 1.0 and 7.5 K. The wet coagulated protofibers were fractured in liquid nitrogen before subjecting them to scanning electron microscopy (SEM) analysis to reveal the cross-sectional features (voids and pores) of the fibers.

Construction of the phase diagram

For constructing the phase diagram at 30°C, the cloud points at various polymer concentrations in DMF were determined by titration. A conical flask with a rubber septum stopper was taken and placed in a constant temperature bath of 30°C. Twenty grams of different concentrations of polymer solutions (polymer + DMF) were taken in the flask. Demineralized water was added into the binary solution with the help of a syringe through the septum, while the polymer solution was continuously stirred using a magnetic stirrer. The titration was considered complete when the first permanent cloud point was obtained. The weight percentages of three components, polymer (P), DMF (S), and water (W), at the cloud point were calculated.

As it was difficult to titrate polymer solution at higher concentrations due to high viscosity, the following procedure was adopted to construct the phase diagram at those concentrations.

Boom et al.[8] has described an approach that describes the concentrations in any single phase that is on the verge of demixing. This is given as follows:

$$\ln\left(\frac{F1}{F3}\right) = b \ln\left(\frac{F2}{F3}\right) + a \quad (1)$$

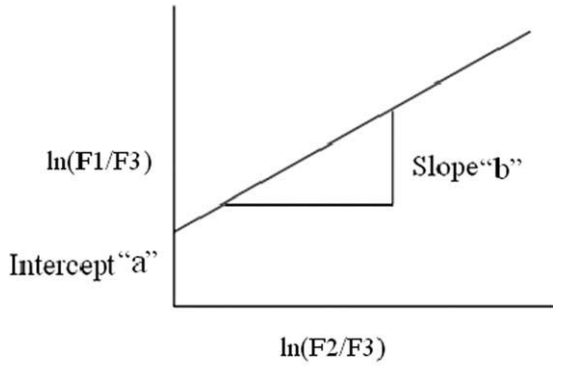

Figure 1 Cloud point line.

where, Fi = weight fraction of component i at the cloud point, a, b are constants 1, 2, 3 represents nonsolvent (W), solvent (S), polymer (P), respectively.

The experimental values were used in eq. (1) and values of constants "a" and "b" were determined by plotting a graph between ln($F1/F3$) vs. ln($F2/F3$) similar to that shown in Figure 1. The intercept gave value of "a" and slope gave value of "b." The values obtained for various polymers are given in Table II.

For different values on "x" axis, corresponding values on "y" axis were taken from the cloud point line of Figure 1 and solved using the following eqs. (2) and (3) for the cloud point compositions on the high polymer concentration side.

$$P = \frac{100}{(1 + e^x + e^y)} \tag{2}$$

$$W/P = e^x \quad \text{and} \quad S/P = e^y \tag{3}$$

These values were used to plot ternary phase diagram using CHEMIX software.

Calculation of interaction parameters

Evaluation of the nonsolvent–solvent interaction parameter χ_{12}

Concentration dependent nonsolvent–solvent interaction parameter χ_{12} is reported in the literature. It is given by the Koningsveld and Kleintjens equation as follows[20]

$$\chi_{12}(\phi_2) = \alpha + \frac{\beta}{(1 - \gamma\phi_2)} \tag{4}$$

where α, β, γ are adjustable parameters, ϕ_2 is volume fraction of solvent in fiber

The values of α, β, γ at different temperatures, as given in the literature,[20] were used for calculating the value of nonsolvent–solvent interaction parameter (χ_{12}) at 32°C. It was calculated to be 0.65. This value was used for all calculations in this article.

Evaluation of water–polymer interaction parameter (χ_{13})

The water–polymer interaction parameters (χ_{13}) for fibers with various compositions were estimated by sorption method.[21] These fibers were immersed in distilled water and after 1 h the fibers were removed and their diameters were measured. This approach was repeated till the fibers reached the equilibrium value i.e., no more swelling occurred in the diameter. The value of polymer–water interaction parameter was calculated based on the average value of water sorption obtained for 5–6 fibers.

The nonsolvent–polymer interaction parameters χ_{13} were evaluated using Flory-Rehner equation.[22]

$$\ln(1 - \phi_3) + \phi_3 + \chi_{13}\phi_3^2 + \frac{v_1\rho}{\overline{M_c}}\left(\phi_3^{\frac{1}{3}} - \frac{1}{2}\phi_3\right) = 0 \tag{5}$$

Here v_1 is the molar volume of nonsolvent, M_c is the average molecular weight between crosslinks, ρ is the density of polymer and ϕ_3 = weight ratio of dried to water swollen film. This equation was originally derived from swelling theory for the crosslinked network. Linear polymer can be considered as a swollen gel with cross links caused by crystalline regions, chain entanglements or van der Waals interactions. The last term was neglected to obtain the following equation because M_c would be quite large for linear polymer[23]

$$\chi_{13} = \frac{-[\ln(1 - \phi_3) + \phi_3]}{\phi_3^2} \tag{6}$$

Weight average and number average degree of polymerization

The number average molecular weight (M_n) was estimated from intrinsic viscosity (refer section "Intrinsic Viscosity") as per the following relation given for poly(acrylonitrile copolymers):

$$M_w = 1.5 \times M_v$$

The weight average molecular weight (M_n) was estimated from M_w assuming the molecular weight

TABLE II
Values of α, β, γ at Different Temperatures

Polymer	a	b
PAN	2.695	0.824
AA10B	2.467	0.781
AA20B	2.395	0.788
AA30B	2.308	0.789
AA40B	2.163	0.783
AA50B	1.943	0.784

TABLE III
Calculations for Weight Average and Number Average Molecular Weights for PAN and its Copolymers

Polymers	Repeat unit (g/mol)	M_v	M_w (= 1.5 × M_v) (g/mol)	X_w	M_n (= M_w/1.7) (g/mol)	X_n
PAN	53	361,492	542,238	10230.9	318,963	6018.7
AA10B	54.9	310,000	465,000	8469.9	213,529	4982.3
AA20B	56.8	340,000	510,000	8978.9	30,000	5281.6
AA30B	58.7	320,000	480,000	8177.1	282,352	4810.1
AA40B	60.6	340,000	510,000	8415.8	300,000	4950.5
AA50B	63.9	360,000	540,000	8450.7	317,647	4971.0

distribution (MWD) of all polymers to be 1.7. MWD of most acrylic copolymers are known to vary in the range of 1.5 to 3.[24,25] The degree of polymerization was calculated by dividing the relevant molecular weight by the repeat unit weight of the respective polymers and copolymers as given in Table III.

Modeling of phase behavior

Assuming that the interaction parameters are independent of polymer molecular weight and concentration, the following equations can be derived for calculating composition at the critical point.[14] Equation (7) is for spinodal and eq. (8) is for binodal curve in a tertiary phase diagram of a polymer–solvent–nonsolvent system.

$$\left(\frac{1}{v_1}+\frac{1}{1-v_1-v_p}-2\chi_{12}\right)\times\left(\frac{1}{v_pX_w^0}+\frac{1}{v_1}-2\chi_{13}\right)-\left(\frac{1}{v_1}+\chi_{23}-\chi_{13}-\chi_{12}\right)^2=0 \quad (7)$$

$$\left[\frac{1}{v_pX_w^0}\left(\frac{1}{v_1^2}-\frac{1}{(1-v_1-v_p)^2}\right)+\frac{1}{v_1^2}\left(\frac{1}{v_2}-2\chi_{23}\right)-\frac{1}{(1-v_1-v_p)^2}\left(\frac{1}{v_1}-2\chi_{13}\right)\right]*\left[\frac{1}{v_pX_w^0}+\frac{1}{v_1}-2\chi_{13}\right]-\left(\frac{1}{v_1}+\chi_{23}-\chi_{13}-\chi_{12}\right)*\left[\frac{1}{v_1^2}\left(\frac{1}{1-v_1-v_p}-2\chi_{23}\right)+\frac{1}{v_1^2v_pX_w^0}+\frac{X_n^0}{v_pX_w^0}\left\{\begin{array}{l}\frac{1}{v_1(1-v_1-v_p)}-\frac{2\chi_{13}}{1-v_1-v_p}-\frac{2\chi_{23}}{v_1}+\\ 2(\chi_{12}\chi_{13}+\chi_{13}\chi_{23}+\chi_{23}\chi_{12})-(\chi_{12}^2+\chi_{13}^2+\chi_{23}^2)\end{array}\right\}\right]=0 \quad (8)$$

where, ν_1 = volume fractions of solvent Polymer.

ν_P = volume fractions of Polymer.

χ_{12} = interaction parameter between non solvent and solvent

χ_{13} = interaction parameter between non solvent and polymer

χ_{23} = interaction parameter between solvent and polymer

X_w^0 = weight average degree of polymerization

X_n^0 = number average degree of polymerization

Evaluation of the solvent–polymer interaction parameter χ_{23}

Using the known values for χ_{12}, χ_{13}, X_w^0, X_n^0, the values of solvent–polymer interaction parameter (χ_{23}) for all polymers were determined by obtaining the best fit of the theoretical binodal point curve to the experimental cloud point curve.

Estimation of critical point composition

For a set of known values of χ_{12}, χ_{13}, χ_{23}, X_w^0, X_n^0, the volumetric concentration at the critical point (ν_1, ν_p) were calculated by solving eqs. (7) and (8), simultaneously, for a common solution using MATLAB version 7.

Sensitivity analysis

For the set of values of parameters χ_{12}, χ_{13}, χ_{23}, X_w^0, X_n^0 for PAN obtained above, the sensitivity of the composition at critical point on these parameters was estimated. For this analysis, each parameter was changed by up to 50% of the PAN value on its either side (positive and negative deviation) while keeping all other parameters constant. The percentage change in the composition at the critical point was plotted against the percentage change in the parameter value under consideration.

RESULTS AND DISCUSSION

Polymer synthesis and composition

A series of acrylonitrile-based copolymers with varying the AAc (acrylic acid content from 0 to 50 mol %) were synthesized by the regulated dosing of the more reactive monomer AAc as reported earlier.[15,16] The addition of AAc in regulated dosing helped in the formation of copolymers with defined architecture as reported earlier.[15,16] The AAc content was found to be close to its feed ratio used during the

TABLE IV
Polymer–Solvent Interaction Parameters (χ_{23}) and Composition at the Critical Points for PAN and its Copolymers

Polymer	Non solvent (water)–solvent interaction parameter χ_{12}	Water–polymer interaction parameter χ_{13}	Solvent–polymer interaction parameter χ_{23}	Composition at the critical point [volume % (weight %)]		
				Water	Solvent	Polymer
PAN	0.65	0.622	0.509	6.8 (6.8)	91.4 (86.46)	2.1 (2.46)
AA10B	0.65	0.612	0.453	8.8 (8.8)	87.95 (83.20)	3.25 (3.77)
AA20B	0.65	0.594	0.405	10.54 (10.54)	85.24 (80.63)	4.22 (4.87)
AA30B	0.65	0.584	0.374	11.25 (11.25)	83.64 (79.12)	5.11 (5.86)
AA40B	0.65	0.55	0.331	12.24 (12.24)	81.01 (76.63)	6.75 (7.68)
AA50B	0.65	0.505	0.313	13.45 (13.24)	78.84 (74.58)	8.01 (9.09)

polymerizations. The composition and various properties of the polymers are given in Tables I and III.

Water–polymer interaction parameter (χ_{13})

The polymer–water interaction parameters for polymers with various compositions were estimated by sorption method in fiber form, the values obtained are tabulated in Table IV.

The water–polymer interaction parameter for poly (acrylonitrile) PAN is 0.622. As the concentration of acrylic acid (AAc) was increased from 10 to 50 mol % in the copolymers, the χ_{13} was found to decrease from 0.612 to 0.505. The polymer–water interaction parameter is known to decrease as the interaction of the polymer and nonsolvent increases. In this case, since the nonsolvent was water, increase in the acrylic acid content increased the hydrophilic nature of the copolymer, and hence, decreased the interaction parameter.

Phase diagrams

Using the values of constant "*a*" and "*b*" from Table II and eqs. (1)–(3), the weight fractions of various components (i.e., polymer, solvent, and water) at cloud points at higher concentrations were estimated. These were used for generating experimental cloud point curves for all the polymers as shown in Figure 2(a–f). The left side of the curve is the miscibility region, while right hand side represents the unstable region, where phase separation takes place.

The experimental curves were fitted using the theoretical bionodal curve equation. All the parameters [χ_{12}, χ_{13}, X_n^0, X_w^0 were known except for solvent–polymer interaction parameter (χ_{23})]. Therefore, value of χ_{23} was varied till the theoretical curve closely matched with the experimental curve for a particular polymer. Similarly, the values of polymer–solvent interaction parameter were estimated for all the polymers. The fitting obtained for the various theoretical binodal curves is shown in Figure 2(a–f) and the corresponding values obtained for χ_{23} are reported in Table IV. As can be seen, all the theoretical curves fitted well for the selected χ_{23} values.

The values of χ_{23} were also found to decrease with increasing content of AAc in the copolymers. The solvent–polymer interaction parameter for PAN was 0.509. It decreased to 0.313 for copolymer with 50 mol % of AAc. The lower value of χ_{23} indicated that modified polymers could interact more strongly with the solvent (for the effect of solvent–polymer interaction in membranes, see Ref. 26).

Because of the higher interaction of the copolymers with both solvent (DMF) and the nonsolvent (water), the cloud point curves shift right towards higher nonsolvent content. This increases the miscibility region of their phase diagram. The effect of interaction parameters on miscibility gap has been reported for membrane inversion coagulation.[9]

The composition of the polymer–DMF-water system at the critical point is given by the intersection of the binodal and spinodal curves. Therefore, it was determined by finding the simultaneous solution of the two theoretical equations given for the two curves. From the various solutions obtained from MATLAB, only those solutions were selected that gave positive values for volume fractions of all three components and yielded summation of the fractions equal to 1.

The polymer content at critical point (C_p) was found to increase steadily as the acrylic acid (AAc) content increased from 0 to 50 mol % in the polymers. For PAN, the concentration of polymer at the critical point (C_p) was found to be 2.1 vol % (2.46 wt %), while it increased by about 400% to a value of 8.01 vol % (9.09 wt %) for copolymer with 50 mol % AAc. The polymer fraction at the critical point (C_p) is possibly the most important parameter that can define the manner in which a polymer phase separates from its solution.

Proposed mechanism of fiber coagulation

According to the phase theory, when a nonsolvent is added slowly to a polymer–solvent solution, the composition of the single-phase solution changes

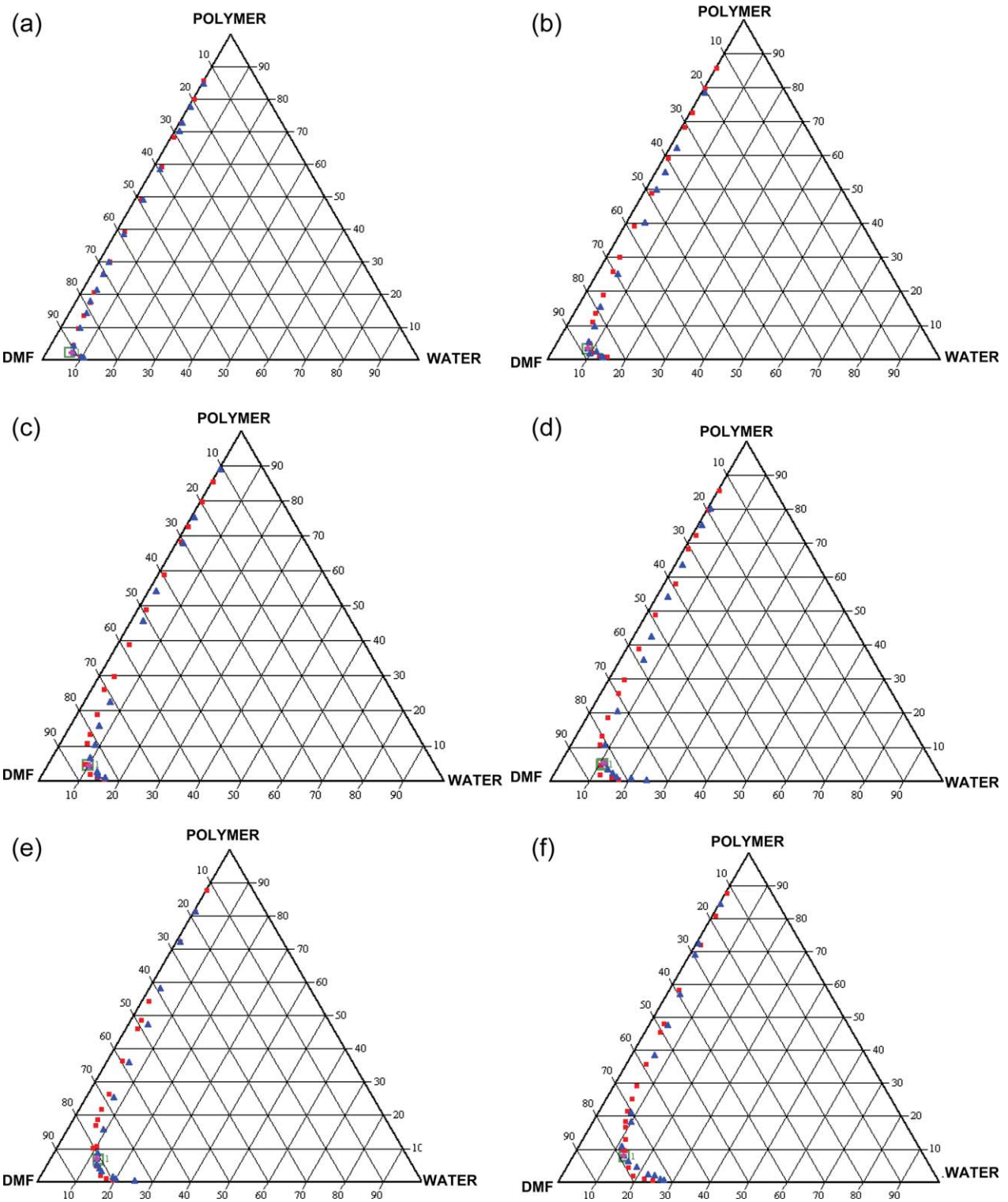

Figure 2 Phase diagram of (a) poly(acrylonitrile) homopolymer, (b) copolymer AA10B, (c) copolymer AA20B, (d) copolymer AA30B, (e) copolymer AA40B (f) copolymer AA50B; experimental bimodal curve, ▲ Theoretical bimodal curve, and critical point. [Color figure can be viewed in the online issue, which is available at wileyonlinelibrary.com.]

gradually until the binodal curve is traversed and the system enters the unstable two phase region of phase diagram. Once it crosses the binodal curve to reach unstable region, the fluctuation in local concentration of the homogeneous phase tend to undergo primary nucleation to form two phases. They are polymer rich phase and polymer lean phases. Out of these two phases, the dispersed

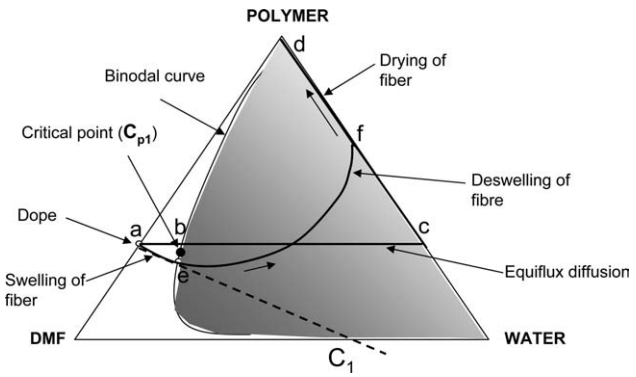

Figure 3 Tertiary phase diagram showing possible paths of coagulation in a wet-spun fiber. Equiflux process "abcd"; nonequiflux process "aefd."

phase is decided by how the polymer solution traverses the binodal curve.[7–11] If it crosses the binodal curve with polymer concentration above the critical concentration "C_p," polymer lean phase is the dispersed phase in the system; whereas, if it crosses below the critical concentration "C_p," polymer rich phase is the dispersed phase. As the phase separation is progressed with further addition of nonsolvent, the primary particles collide and amalgamate with each other and grow into larger particles called secondary particles, which further amalgamate to create coagulated structure. If the polymer rich phase is dispersed phase, on amalgamation it forms a homogeneous network of polymer chains. On the other hand, if the polymer lean phase is dispersed, it forms large and small voids entrapped in the matrix of the polymer.

During coagulation of a freshly extruded fiber, the nonsolvent moves in and the solvent moves out at the same time, and the situation is a bit different than described above, where nonsolvent is continuously added to a polymer solution. However, the result of the coagulation of a fiber is similar to the

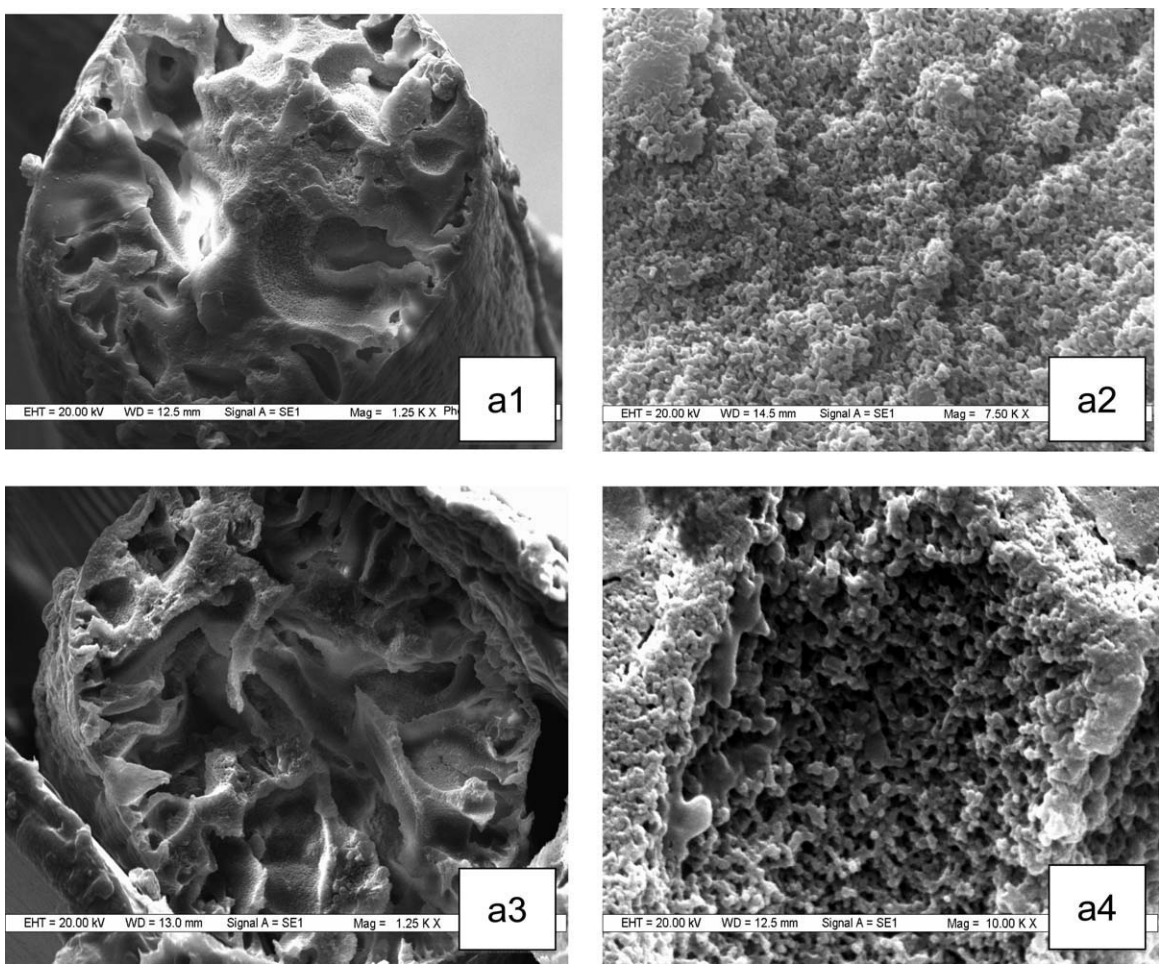

Figure 4 Scanning electron micrographs of cross-sections of protofibers: Effect of polymer dope concentration on the morphology of fibers; (a) AA10B, coagulation bath 10% DMF (a1) 10 wt % dope, magnification ×1250; (a2) 10 wt % dope, magnification ×7500; (a3) 20 wt % dope, magnification ×1250; (a4) 20 wt % dope, magnification ×10,000; (b) AA20B, coagulation in 30% DMF (b1) 10 wt % dope, magnification ×1250; (b2) 10 wt % dope, magnification ×5750; (b3) 20 wt % dope, magnification ×1250; (b4) 20 wt % dope; magnification ×7500.

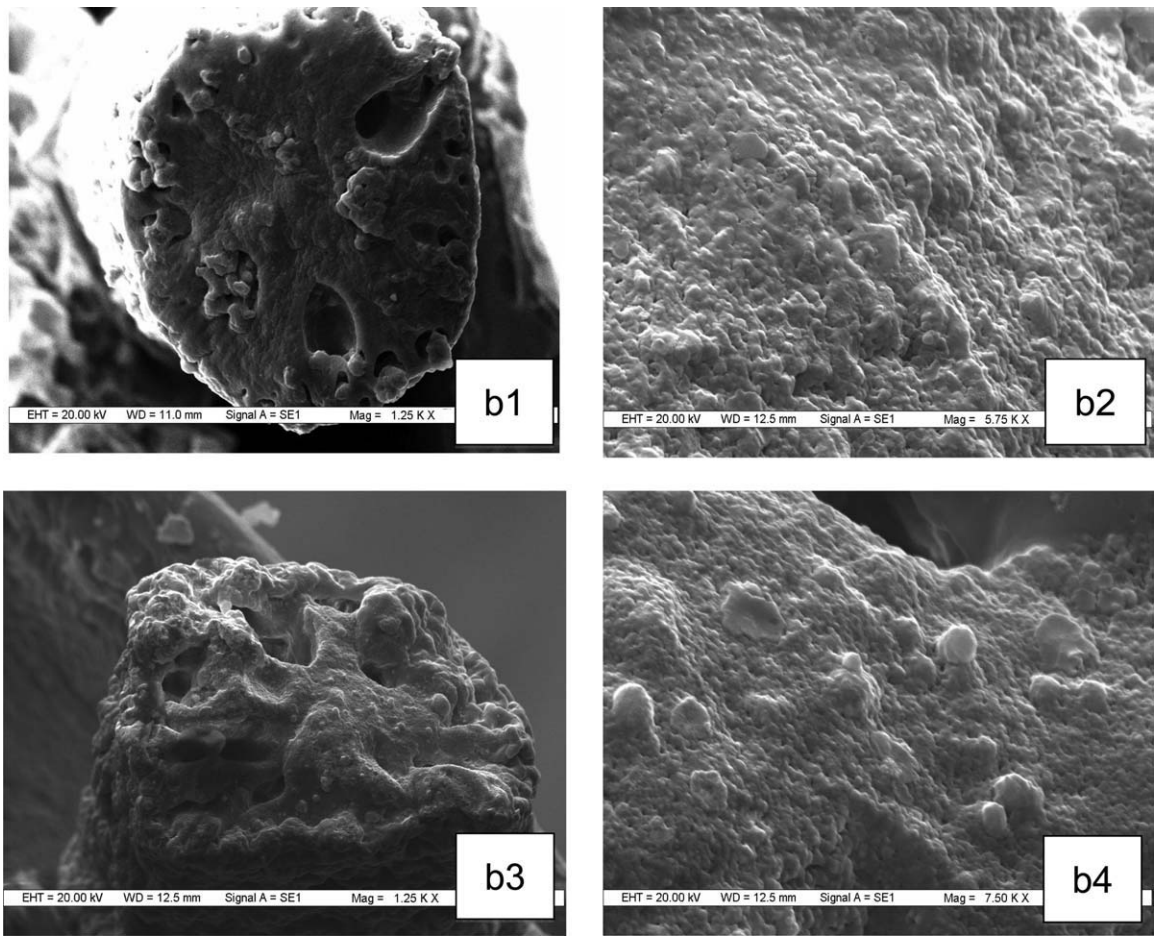

Figure 4 (*Continued from the previous page*)

above in the manner that the composition inside the fiber changes and it crosses from miscible to immiscible region (i.e., from the left side to the right side of the binodal curve) as coagulation proceeds.

It would be interesting to investigate what effect does the thermodynamics of phase separation has on the morphology of the protofiber when a freshly extruded polymer dope solution in a fiber form is coagulated.

Effect of polymer dope concentration on the protofiber morphology

It is normally stated that the fibers solution spun from higher polymer concentration tend to give more homogeneous fibers,[1–4] however, if the phase theory is applicable to the fiber coagulation, the effect should be exactly opposite.

During coagulation in wet spinning, if we assume that the coagulating fiber does not swell or deswell, then the concentration of the polymer phase should remain constant till the coagulation is complete. This case is similar to equiflux situation, where the rate of diffusion of solvent out of the fiber is equal to the rate of diffusion of nonsolvent into the fiber. When the coagulation is complete, the fiber is left with only two components polymer and nonsolvent, and then it approaches pure polymer as it is dried. This path "abcd" is shown in Figure 3.

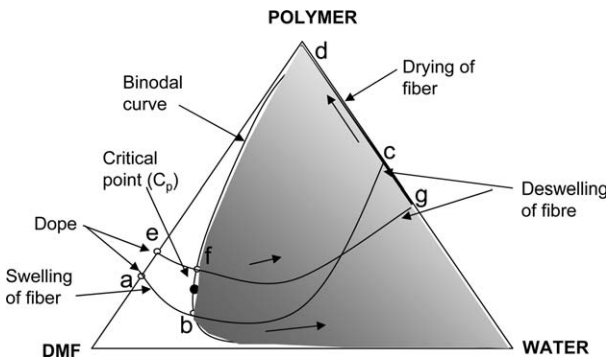

Figure 5 Tertiary phase diagram showing possible paths of coagulation in a wet-spun fiber (a) lower dope concentration path "abcd" (b) higher dope concentration path "efgd".

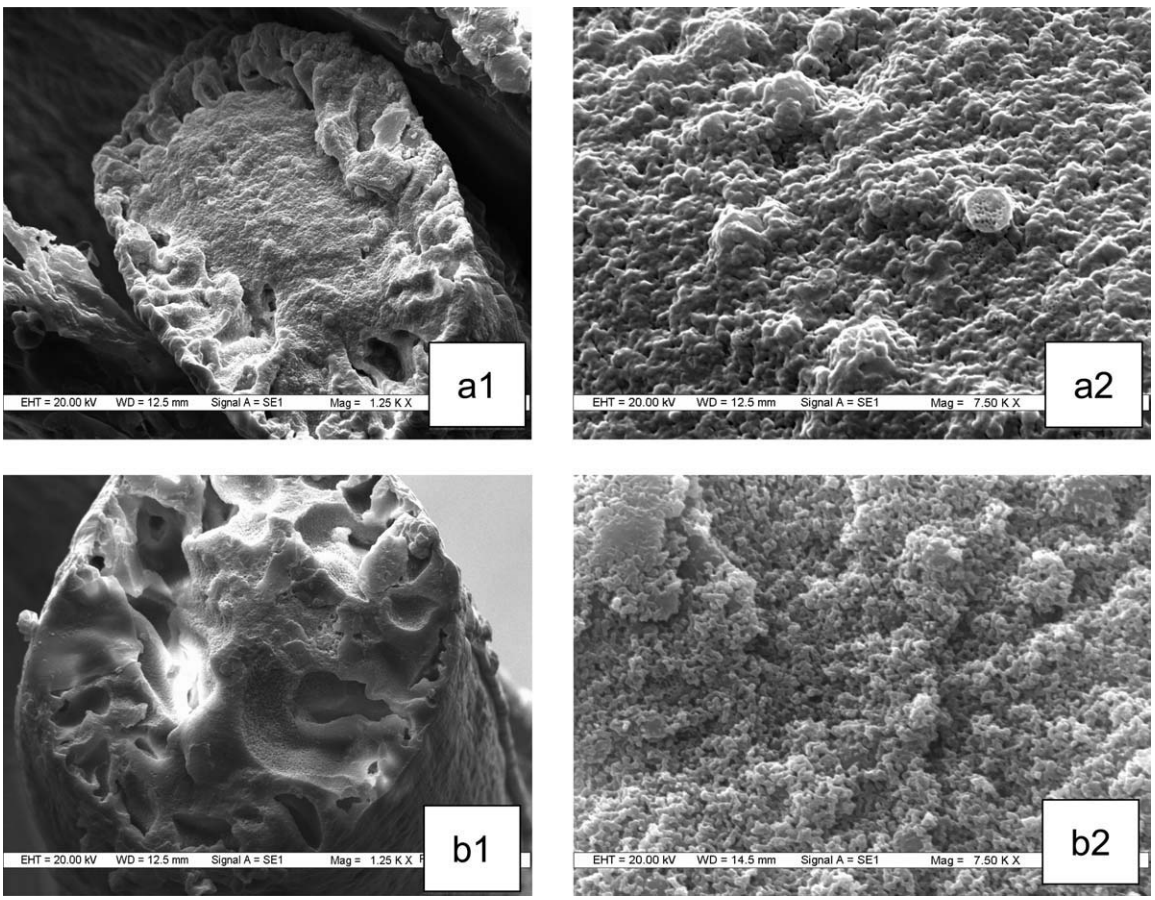

Figure 6 Scanning electron micrographs of cross-sections of protofibers: Effect of coagulation bath concentration on the morphology of fibers; AA10B, 10 wt % dope concentration (a1) coagulation bath of 30% DMF, magnification ×1250; (a2) coagulation bath of 30%, magnification ×7500; (b1) coagulation bath of 10% DMF, magnification ×1250; (b2) coagulation bath of 10% DMF, magnification ×7500.

In the above situation, the fiber is likely to take coagulation path below the critical point, C_{p1}, if the concentration of dope is lower than the critical concentration. If the dope concentration is above the critical concentration, the coagulation path is likely to cross the binodal curve above the critical point (as shown in Fig. 3). However, the C_{p1} for PAN is only 2.46 wt%, therefore; only very dilute solutions of PAN are likely to generate void free homogeneous fibres. Spinning fibers from such dilute polymer concentrations are nearly impossible for PAN with the given molecular weight.

Fortunately, the fibers have been shown to swell to a large extent (by 200–250% by volume) during the initial phases of coagulation,[13] wherein the nonsolvent enters the fiber. This is similar to the situation, where, nonsolvent is added to a polymer solution. This is likely to force the fiber composition to take path towards the solvent–nonsolvent line before the fiber starts to collapse. Once the fiber starts to collapse, the flux of solvent coming out becomes significantly higher than the flux of nonsolvent entering into the coagulating fiber. This is likely to give an upside turn to the coagulation path (aefd) as shown in Figure 3. However, the initial swelling "ae" of protofiber may bring down the polymer composition of the fiber by about 50%, and this enables fibers to follow a coagulation path that passes below or near the critical point C_{p1} even when they are spun at relatively higher dope concentrations.

To investigate the effect of dope concentration on the morphology of the solution spun protofibers, it was decided to solution spin fibers from two concentrations 10 and 20 wt % of AA10B in DMF. The cross-section of these fibers under SEM is shown in Figure 4(a). Clearly from the figure, both the fibers have several large voids possibly because the polymer concentrations were much higher than the critical point. However, the fiber solution spun from lower polymer dope concentration had significantly smaller and fewer voids compared to the other fiber. Also, when the solid part of the fibers was further magnified, it showed more dense structure (less porosity) in fibers spun from lower dope concentration. This was found

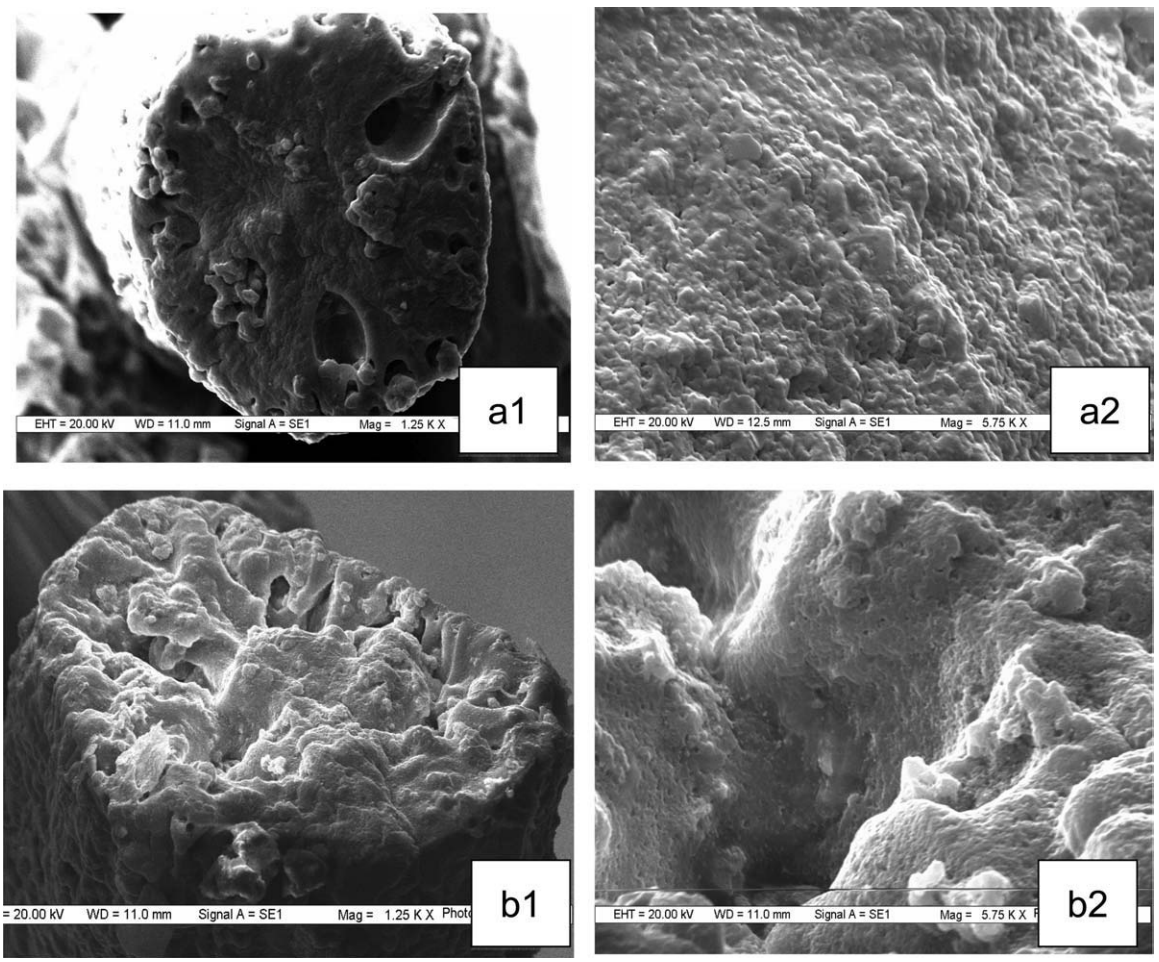

Figure 7 Scanning electron micrographs of cross-sections of protofibers: Effect of coagulation bath concentration on the morphology of fibers; AA20B, 10 wt % dope concentration (a1) coagulation bath of 30% DMF, magnification ×1250; (a2) coagulation bath of 30% DMF, magnification ×5750; (b1) coagulation bath of 10% DMF, magnification ×1250; (b2) coagulation bath of 10% DMF, magnification ×5750.

to be true for all polymers (AA10B, AA20B) that could be spun using the low concentration of 10 wt % [Figure 4(a,b)]. The fibers could not be spun from polymer concentration lower than 10 wt %.

Figure 5 shows the possible explanation for the above observations. The fibers formed from lower polymer dope concentration were likely to cross-over to the phase separation region either below

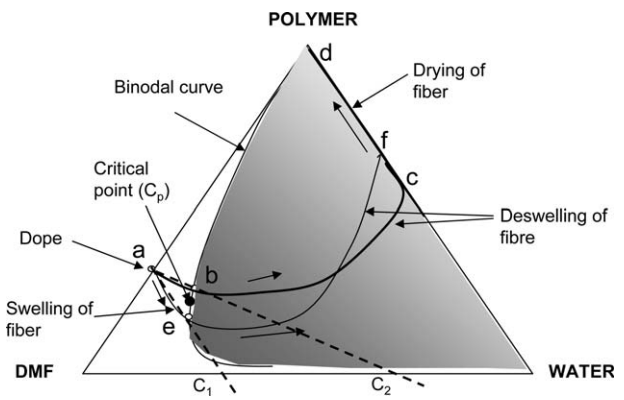

Figure 8 Tertiary phase diagram showing possible paths of coagulation in a wet-spun fiber (a) lower coagulation bath concentration C_2, path "abcd" (b) higher coagulation bath concentration C_1, path "aefd".

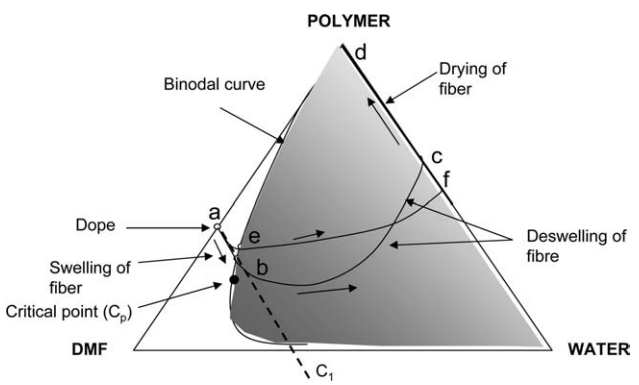

Figure 9 Tertiary phase diagram showing possible paths of coagulation in a wet-spun fiber (a) lower coagulation-bath temperature, path "abcd" (b) higher coagulation bath temperature, path "aefd".

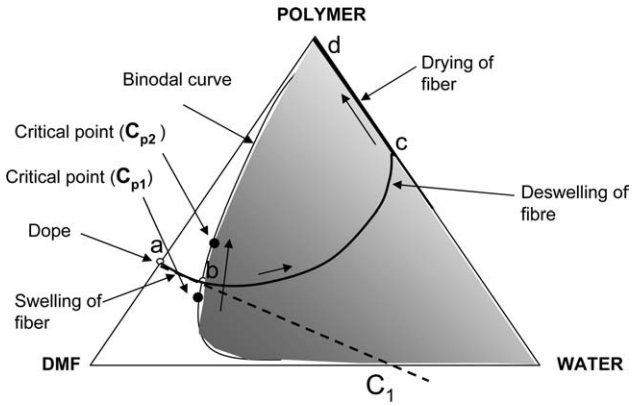

Figure 10 Tertiary phase diagram showing the effect of critical point on the possible path of coagulation in a wet-spun fiber (a) path "abcd" passes above C_{p1} (b) path "abcd" passes below C_{p2}.

(path "abcd") or much nearer to the critical point than the other (path "efgd"), and therefore, had coagulated into a more homogeneous, denser structure with fewer large voids.

Effect of coagulation bath concentration on protofiber morphology

Figures 6 and 7 show the effect of coagulation bath concentration on the morphology of the protofibers AA10B and AA20B. The coagulation bath condition was modified from 90 : 10 :: water : DMF to 70 : 30 :: water : DMF (v/v). When the spinning was carried out at higher bath concentration (30% DMF), the fiber cross-section has much fewer and smaller voids. These voids are only located towards the periphery and the core is more homogeneous. The solid portion is also comparatively denser than the fiber spun at lower (10% DMF) bath concentration.

The effect of coagulation bath concentration has been principally explained on the kinetics of coagulation in the literature.[1–3,27] According to kinetic effect, at a higher bath concentration (i.e., high solvent in solvent–nonsolvent mixture), the concentration gradient is lower between the fiber and the bath, which leads to slower diffusion flux and a more homogeneous structure. However, the physical

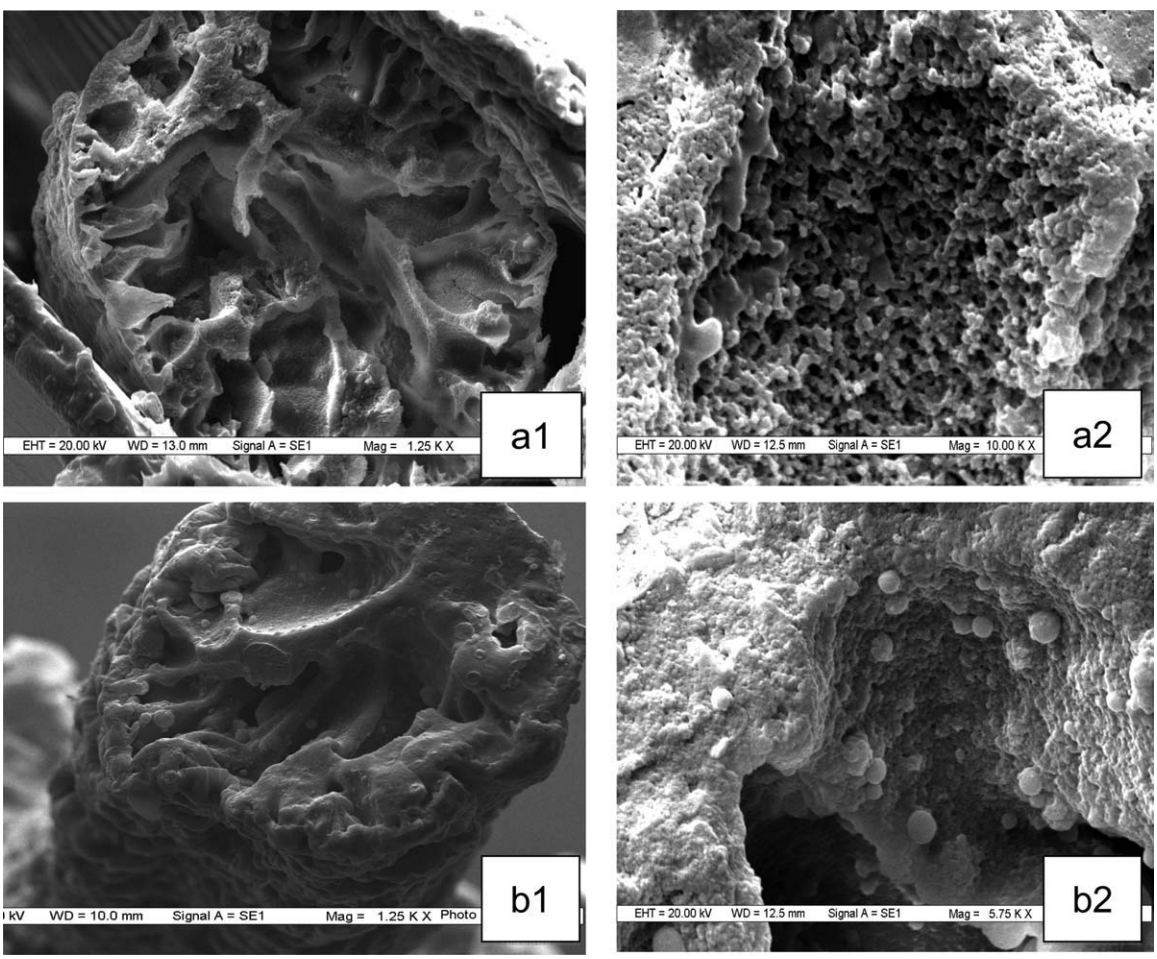

Figure 11 Scanning electron micrographs of cross-sections of protofibers: Effect of acrylic acid content on the morphology of fibers; coagulation bath concentration 10% DMF, dope concentration 20 wt % (a1) AA10B, magnification ×1250; (a2) AA10B, magnification ×10,000, (b1) AA20B, magnification ×1250; (b2) AA20B, magnification ×5750; (c1) AA30B, magnification ×1250; (c2) AA30B, magnification ×4050; and (d1) AA50B, magnification ×1250; (d2) AA50B, magnification ×5750. [Color figure can be viewed in the online issue, which is available at wileyonlinelibrary.com.]

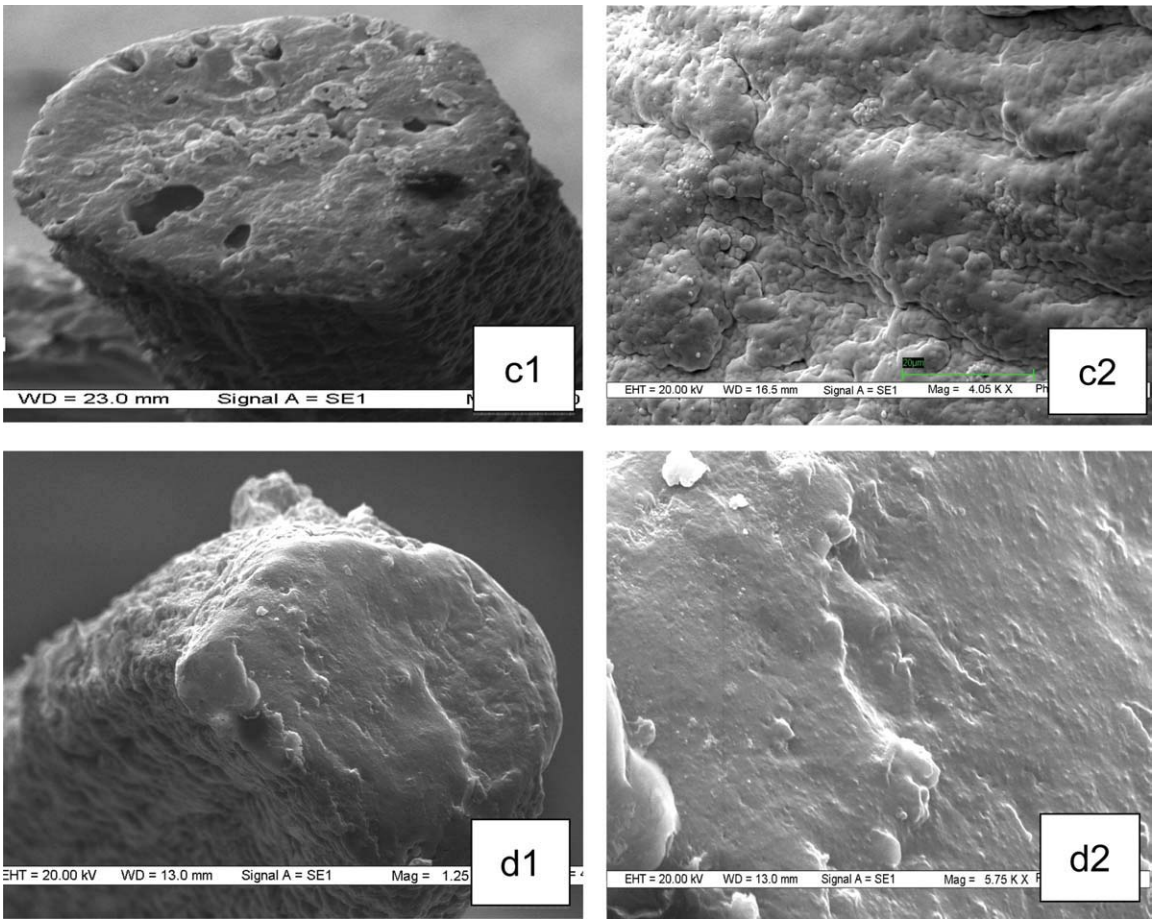

Figure 11 (*Continued from the previous page*)

state of the system (coagulated fiber) must be principally decided by the thermodynamics and not the kinetics of the process.

The effect of spinning of the fibers at higher bath concentration may be explained on the basis of the variation in compositional path of the coagulating fiber during the process. As mentioned earlier, the initial swelling of fibers can allow a situation, where a fiber spun from higher polymer dope concentration than C_p may follow a coagulation path into the unstable region nearer to the critical point compared to the situation if swelling would have not taken place. In such a situation, deviation of the coagulation path towards solvent–nonsolvent line would depend on the concentration of coagulation bath. As is depicted in Figure 8, the fiber may take path "aefd" (i.e., below the critical point) or "abcd" (i.e., above the critical point) depending upon the coagulation bath concentration. If bath concentration is kept high at C_1, path "aefd" is likely to be below the critical point; otherwise it is above the critical point.

In our case, the fibers spun at 30% (v/v) bath concentration also show some voids, therefore, it is likely that the path is still above the critical point, though it may be passing over to phase separation region at much nearer to the critical point than the fiber spun in 10% bath concentration.

Effect of coagulation temperature on protofiber morphology

The other process parameter, which according to the reported literature, is considered to change the kinetics, and hence, the morphology of a coagulating fiber is "temperature of coagulation." Again, the explanation of developing morphology must be based on thermodynamics of the process rather than the kinetics. Several studies[1–3] have reported formation of larger and more number of voids when PAN is wet spun at a higher temperature compared to a lower.

This may be explained as different paths taken by the fibers when coagulated at different temperatures as shown in Figure 9. As mentioned above, the composition of the fiber moves towards solvent–nonsolvent line due to the swelling effect at the initial phase of coagulation. During this phase, the nonsolvent diffuses in and the diameter of the fiber increases considerably (beyond the extrudate swell point). It has also been reported that the extent of

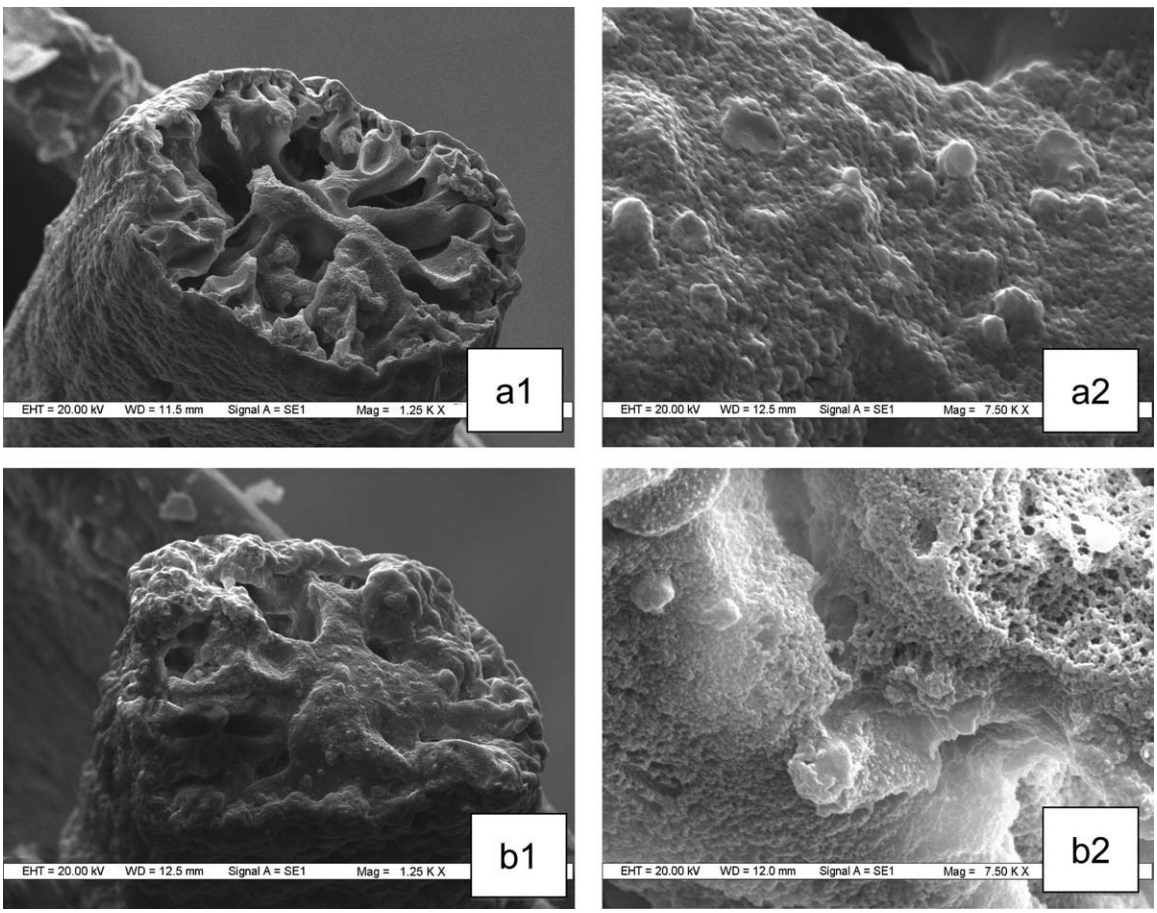

Figure 12 Scanning electron micrographs of cross-sections of protofibers: Effect of acrylic acid content on the morphology of fibers; coagulation bath concentration 30% DMF, dope concentration 20 wt %: (a1) AA10B, magnification ×1250; (a2) AA10B, magnification ×7500, (b1) AA20B, magnification ×1250; (b2) AA20B, magnification ×7500; (c1) AA30B, magnification ×1250; (c2) AA30B, magnification ×5750; and (d1) AA50B, magnification ×1250; (d2) AA50B, magnification ×5750. [Color figure can be viewed in the online issue, which is available at wileyonlinelibrary.com.]

swelling is a strong function of temperature of coagulation.[13] At lower temperature, the swelling is high (up to 250% by volume), i.e., deviation of compositional path towards solvent–nonsolvent line continues for a larger extent, and the coagulating fiber may take a path given by "abcd." At higher temperature of coagulation, the swelling is considerably lower (110–120% by volume), and therefore, the deviation is expected to be much lower giving rise to compositional path during coagulation as "aefd." Path "abcd" passes much nearer to the critical composition than path "aefd," and hence, is expected to give structure with small and fewer voids.

Additionally, the phase diagram is defined only at a given temperature and pressure, and it changes with the change in temperature. At lower temperature, the cloud point curve should move to the right toward nonsolvent axis, giving a larger miscibility region. This would allow the protofiber slightly more time to swell giving compositional path "abcd" as explained above. However, in this study, experimental cloud point curves did not appear to vary considerably with small changes in titration temperature (5–10°C).

Effect of critical point composition on the protofiber morphology

In the earlier studies for the system PAN–DMF-water, critical point was found to lie at a very low value which suggested that a very low polymer dope concentration is required to be used for void free spinning. However, this is undesirable as it would be difficult to spin and would also lower the productivity of spinning line. Therefore, it is important that the PAN–DMF-water system should be modified such that critical point for the polymer–solvent–nonsolvent system can be moved up towards the higher polymer concentration. As shown in Figure 10 if the critical point can be moved from a lower critical polymer concentration "C_{p1}" to higher critical polymer concentration "C_{p2}," then dope solution with higher polymer concentration may be used to obtain coagulation path below the critical point.

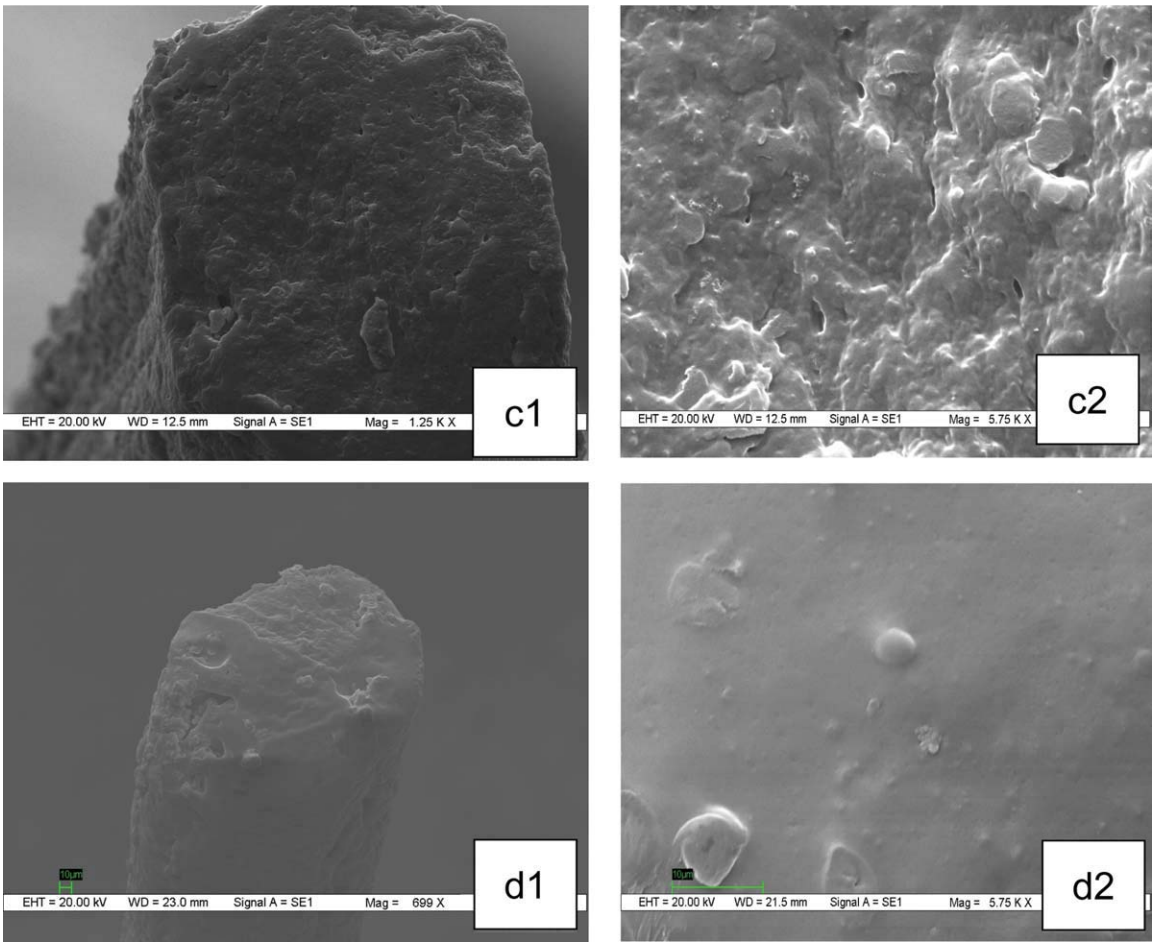

Figure 12 (*Continued from the previous page*)

Dispersion of polymer rich phase would allow formation of dense and void free morphology.

In the series of copolymers from PAN to AA50B, the polymer concentration at the critical point could be increased about four times from 2.46 to 9.09 wt %. This should allow us to spin homogenous fibers at high polymer dope concentration. Figure 11 shows morphology of fibers from AA10B to AA50B spun at 20 wt % dope concentration in a bath of 30% (v/v). From the figures, it can be seen that as the critical point of the polymer–DMF–water system moves up toward the polymer vertex, there is a dramatic decrease in the number and size of the voids. Also, the structure has become denser. For fibers from AA30B, the number of voids or pores are negligible, while in fibers from AA50B, the fiber is completely compact without any voids. The results indicate that spinning the fiber from AA50B even with high dope concentration (20 wt %) and into the bath of low concentration (10% DMF), the morphology could be significantly improved to a compact structure. It is important to note that all the above fibers were spun at 30°C, at which the PAN fibers are known to show high degree of void formation due to rapid rate of coagulation.[2]

The morphology of the fibers spun from AA10B, AA20B, AA30B, and AA50B into a coagulation bath

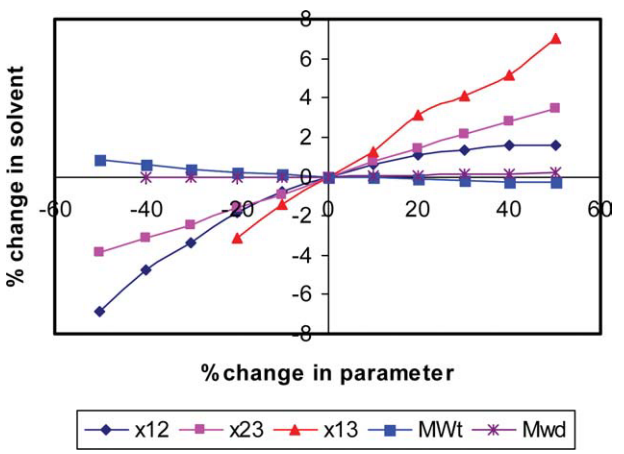

Figure 13 Sensitivity analysis of various parameters on the % change in solvent content at the critical point. [Color figure can be viewed in the online issue, which is available at wileyonlinelibrary.com.]

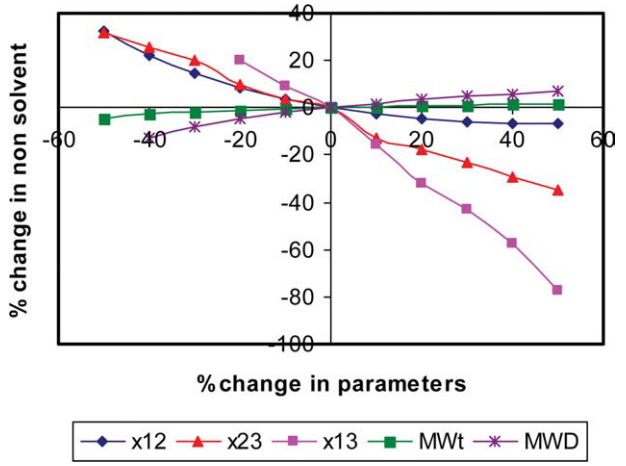

Figure 14 Sensitivity analysis of various parameters on the % change in nonsolvent content at the critical point. [Color figure can be viewed in the online issue, which is available at wileyonlinelibrary.com.]

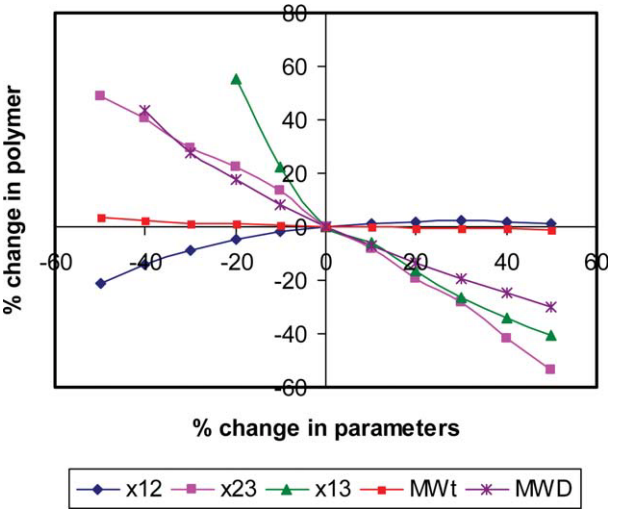

Figure 15 Sensitivity of various parameters on the % change in polymer content at the critical point. [Color figure can be viewed in the online issue, which is available at wileyonlinelibrary.com.]

with higher concentration (30% DMF) is shown in Figure 12. Again, in this set of samples, the morphology of fibers improves as the acrylic acid content in the fibers increases and a very compact structure is obtained for fibers from AA50B.

Compared to the morphology of fibers spun at lower bath concentration (10%DMF), the morphology of fibers spun in higher bath concentration is more homogeneous, denser and having fewer large voids. This difference, due to spinning in higher bath concentration, is clearly evident for fibers from AA10B, AA20B, and AA30B. However, interestingly, the morphology of fibers from AA50B is very similar (i.e., dense and void free) to that spun into the bath of lower concentration (Figure 11). It may be inferred that changes brought about in the phase behavior (i.e., higher critical point C_p) of the polymer AA50B are sufficient to produce fibers with a compact, homogeneous void free morphology.

Sensitivity analysis of parameters

Sensitivity analysis of the various parameters [χ_{12}, χ_{13}, χ_{23}, X_w^0 Molecular weight distribution (MWD)] associated with phase behavior was performed in order to understand the importance of various parameters on the composition of the critical point in a polymer–solvent–nonsolvent tertiary system. This analysis would help in designing new polymer structures or modifying the existing one so that desirable structures may be produced on wet spinning.

Figure 13 shows the effect of various parameters, χ_{12}, χ_{13}, χ_{23}, X_w^0, MWD, on the solvent content at the critical point. Interestingly, weight average molecular weight does not have any appreciable effect on its composition. The percentage changes in solvent content are small for all parameters because the solvent is present in large quantity at the critical point. However, it is mostly affected by the interaction parameters and not so much with molecular weights or their distribution.

Similarly, the nonsolvent content at the critical point is affected by solvent–polymer interaction (χ_{23}) and water–polymer interaction (χ_{13}) parameters. Figure 14 shows the effect of parameters on the nonsolvent content at the critical point. With the improved

TABLE V
Effect of Acrylic Acid Content on Coagulation Time and Maximum Stretching During Coagulation of Fibers from PAN and its Copolymers

	(90 : 10 :: Water : DMF) (v/v)		(70 : 30 :: Water : DMF) (v/v)	
Polymer	Time of coagulation (s)	Coagulation bath stretch	Time of coagulation (s)	Coagulation bath stretch
Pure PAN	Instantly	1	10–15	1.5
AA10B	10–12	1.73	30–40	2.3
AA20B	35–38	2.9	56–58	4.5
AA30B	48–50	3.2	70–80	5.7
AA40B	60–63	4	120	6.8
AA50B	80–85	4.3	120–150	7.6

interaction of the water with the polymer, its concentration increases most significantly. Again, molecular weights or their distribution does not have any significant effect on the nonsolvent (water).

Figure 15 shows the effect of various parameters on the polymer composition at the critical point (C_p). The polymer content is sensitive to many parameters and changes very strongly with its interaction with solvent and nonsolvent. As these interactions improve (i.e., χ_{13} and χ_{23} decrease), the polymer content at the critical point increases. With water, it increases sharply. Interestingly, molecular weight distribution (MWD) has significant effect on the coagulation behavior of the polymer. Broader distribution lowers the polymer content while narrower distribution increases it (C_p). Therefore, keeping a lower molecular weight distribution would help in obtaining a homogeneous, compact structure of fibers even when spun from higher dope concentration. On the other hand, value of the molecular weight and solvent–nonsolvent interaction parameters have negligible effect on the polymer content.

Though molecular weight in the range tested above, did not seem to affect the phase diagram or the composition of the critical point, it can not be generalized for all molecular weights. Phase diagrams for polymers with very low molecular weights or for systems with very low polymer concentrations may have significant dependence on the changes in molecular weight.[28,29]

Effect of acrylic acid on spinnability

As the acrylic acid content increased in the copolymers, values of their two interaction parameters, χ_{23} (solvent–polymer interaction parameter), and χ_{13} (nonsolvent–polymer interaction parameter) decreased. The increase in the compatibility between polymer and diluent (DMF), which was reflected by the decrease in the interaction parameter "χ_{23}," was found to shift the location of the binodal curve to the right, thereby, increasing the miscible region. Also, the increase in the interaction of polymer with nonsolvent (water) has further helped in increasing the miscibility region and decreasing the precipitation tendency of the copolymers.

This increase in miscibility region is expected to have direct impact on the spinning behaviour of the copolymers. The spinnability of a polymer is defined as its ability to get extended irreversibly under the tensile stress. This is normally determined in terms of the amount of stretch the polymer can be imparted in the coagulation bath. Higher the stretch, more is the spinnability. Table V shows the values of maximum stretch the spinning fibers can be imparted in the coagulation bath along with the time it takes to coagulate. The fibers from copolymers with higher AAc content showed slower rate of coagulation and could be stretched to significantly higher value.

Higher maximum stretch in the coagulation bath, which is a function of the maximum jet-stretch that can be given to a fiber, may allow spinning of finer fibers with better mechanical properties.

From the above results, it can be inferred that thermodynamic consideration during coagulation of wet spun fibers is the primary factor that decides the internal structure of the protofiber.

CONCLUSIONS

Thermodynamics play an important role in determining the phase behaviour of a three component (tertiary) system such as polymer–solvent–nonsolvent. This in turn should affect the coagulation behavior of the solution spun fibers. To investigate this behaviour, a series of poly(acrylonitrile–*co*-acrylic acid) copolymers were synthesized. Using titration method and extrapolation, the phase diagrams of these copolymers in DMF-water system were developed. Using these experimental binodal curves, interaction parameters and the composition of system at the critical point were determined as a function of AAc content in the copolymers.

The effect of various process parameters on the thermodynamics and the subsequent morphology of the protofibers has been investigated. The structure of protofibers from acrylonitrile copolymers was found to be greatly influenced by the composition path it takes during coagulation while passing from miscible to immiscible region of the phase diagram. If the polymers were spun from higher dope concentration, they took a path above the critical polymer concentration and developed a porous structure with large voids, while if they were spun from lower dope concentration, vice versa was true. This observation was contrary to the general belief that higher dope concentration gives more homogeneous fibers.

Similarly, the coagulation bath concentration appeared to influence the path of coagulation and the morphology of the protofibers. At higher coagulation bath concentration, the coagulating path took a deviation more towards the solvent–nonsolvent line and tended to pass near the critical point giving rise to a denser structure. A similar thermodynamic explanation has been provided for obtaining a denser fiber when the polymer is spun at lower coagulation bath temperature than higher. At lower temperature, the fiber swelling is higher which leads to compositional path closer to the critical point.

On the other hand, chemical modification of the PAN with acrylic acid comonomer could significantly alter the phase behavior and the morphology of the protofibers. It was found that with increase in

the AAc content, both the solvent–polymer (χ_{23}) and water–polymer (χ_{13}) interaction parameters decreased and the region of miscibility of the system increased. The critical point composition also changed dramatically with the AAc content and the critical polymer concentration (C_p) could be increased by almost 400% in going from PAN to copolymer with 50% AAc. Because of the changes brought about in the phase behavior, the fibers from copolymers with higher AAc content could be spun into dense structures even at adverse spinning conditions such as high dope concentration, low coagulation bath concentration and high temperature of spinning.

Finally, it could be concluded that the coagulation path (i.e., change in composition inside the fiber during coagulation) taken by the fiber in going from miscible to immiscible region appeared to be the fundamental and the most critical factor that decides the morphology of the protofiber. Because of any reason, if the fiber takes coagulation path above the critical polymer concentration, void filled structure is produced, while if it takes coagulation path near or below the critical polymer concentration, denser structure without voids could be easily produced. This understanding in wet spinning of polymers may help in producing fibers with desirable morphology and mechanical properties.

References

1. Craig, J. P.; Knudsen, J. P; Holland, V. F. Text Res J 1962, 32, 435.
2. Knudsen, J. P. Text Res J 1963, 33, 13.
3. Takahashi, M.; Nukushina, Y.; Kosugi, S. Text Res J 1964, 34, 87.
4. Bajaj, B.; Sengupta, A. K.; Jain, P. C. Text Res J 1980, 218–223.
5. East, G. C.; McIntyre, J. E.; Patel, G. C. J Text Inst 1984, 3, 196.
6. Baojun, Q.; Jian, Q.; Zhenlong Z. Text Asia 1989, No. 5, 3, 32, 49–51 .
7. Mulder, M. H.V. Basic Principles of Membrane Technology. Amsterdam: Elsevier, 1991.
8. Boom, R. M.; Van den Boomgaard, T.; van den Berg, J. W. A.; Smolders C.A. Polymer 1993, 34, 2348.
9. Wei, Y.-M.; Xu, Z.-L.; Yang, X.-T.; Liu, H.-L. Desalination 2006, 192, 91.
10. Kamide, K.; Iijima, H.; Matsuda, S. Polym J 1993, 25, 1113.
11. Iijima, H.; Matsuda, S.; Kamide, K. Polym J 1994, 26, 439.
12. Law, S. J.; Mukhopadhyay, S. K. J Appl Polym Sci 1997, 65, 2131.
13. Law, S. J.; Mukhopadhyay, S. K. J Appl Polym Sci 1998, 69, 1459.
14. Kamide, K.; Matsuda S. Polym J 1986, 18, 47.
15. Sahoo, A.; Jassal, M.; Agrawal, A. K. J Appl Polym Sci, 2007, 105, 3171–3182.
16. Sahoo, A.; Ramasubramani, K. R. T.; Jassal, M.; Agrawal, A. K. Eur Polym J 2007, 43, 1065.
17. Bandrup, J.; Immergut, E. H.; Grulke, E. A. Polymer Handbook, 4th ed., New York: John Wiley, 1999; Chapter VII-11.
18. Brar, A. S.; Dutta K. Eur Polym J 1998, 34, 1585.
19. Bajaj, P.; Sreekumar, T. V.; Sen, K. J Appl Polym Sci 2001, 79, 1640.
20. Yilma, Z. L.; McHaugh, A. J. J Appl Polym Sci 1986, 31, 997.
21. Lee, H. K.; Kim, J. Y.; Kim, Y. D.; Shin, J. Y.; Kim S. C. Polymer 2001, 42, 3893.
22. Flory, P. J.; Rehner J. Chem Phys 1943, 11, 521.
23. Mulder, M. H. V.; Smolders, C. A. J Membr Sci 1984, 11, 521.
24. Gupta, V. B.; Kothari, V. K. Manufactured Fibre Technology; Chapman and Hall: London, 1990; pp 406–453.
25. Cha, C. Y. Polym Lett 1969, 7, 343.
26. Gaides, G. E.; Mc Hugh, A. J. Polymer 1989, 30, 2118.
27. Um, I. C.; Kweon, H. Y.; Lee, K. G.; Ihm, D. W., Lee, J. H.; Park, Y. H. Int J Biol Macromol 2004, 34, 89.
28. Phadke, M. A.; Kulkarni, S. S.; Karode, S. K.; Musale, D. A. J Polym Sci Part B: Polym Phys 2005, 43, 2074.
29. Kim, J. Y.; Lee, H. K.; Baik, K. J.; Kim, S. C. J Appl Polym Sci 1998, 65, 2643.